

Transactions of the VŠB – Technical University of Ostrava, Mechanical Series

No. 1, 2010, vol. LVI

article No. 1760

Václav KRYS*, Milan MIHOLA, Petr NOVÁK*****

MANIPULATION SUBSYSTEM OF HERCULES MOBILE ROBOT

MANIPULAČNÍ SUBSYSTÉM MOBILNÍHO ROBOTU HERCULES

Abstract

The article describes a manipulation subsystem for the mobile robot HERCULES. The manipulator was designed and realized on the Department of robotics as a part of the MPO project “VÝZKUM A VÝVOJ SPECIÁLNÍHO VÍCEÚČELOVÉHO ZÁSAHOVÉHO VOZIDLA“ with registration number FT-TA3/014 at which we participated. In the article is described the drive unit which was designed for the joints of the manipulator. Further is described methodology of functional tests which were done for verification of functional parameters and their comparison with parameters obtained from simulations on virtual prototypes.

Abstrakt

V článku je popsán manipulační subsystém mobilního robotu HERCULES. Manipulátor byl navržen a realizován na Katedře robototechniky v rámci řešení etapy projektu MPO „VÝZKUM A VÝVOJ SPECIÁLNÍHO VÍCEÚČELOVÉHO ZÁSAHOVÉHO VOZIDLA“ s evidenčním číslem FT-TA3/014 jehož jsme byli spoluřešitelé. V článku je dále popsána pohonná jednotka, která byla pro potřeby manipulátoru navržena. V závěru článku je popsána metodika funkčních testů manipulátoru pro ověření funkčních parametrů a jejich srovnání s parametry získanými při výpočtech a simulacích na virtuálních prototypch.

1 INTRODUCTION

The described manipulator is a subsystem of the Mobile Robot (MR) HERCULES realized on the Department of Robotics as a part of a project at which we participated. Conceptual designs and preliminary cost analysis of the mobile robot undercarriage were done in accordance to specified requirements. A search for available and suitable commercial platforms for MR undercarriages was accomplished at the same time. Development and production of an undercarriage of our own design as well as purchase of commercial platform were found to be too expensive. Purchase of a motorized wheelchair with desired values of travel range, speed and loading capacity and its rebuilding into a MR showed to be the proper solution. Manipulation subsystem, visual subsystem and universal portable operator control unit were designed and realized on our department, as well as control unit, software and user interface application for robot remote control.

* Ing., VŠB - Technical University of Ostrava, Faculty of Mechanical Engineering, Department of Robotics, 17. listopadu, 70833, Ostrava-Poruba, tel. (+420) 59 732 5310, e-mail: vaclav.krys@vsb.cz

** Ing., VŠB - Technical University of Ostrava, Faculty of Mechanical Engineering, Department of Robotics, 17. listopadu, 70833, Ostrava-Poruba, tel. (+420) 59 732 5445, e-mail: milan.mihola@vsb.cz

*** prof. Dr. Ing., VŠB - Technical University of Ostrava, Faculty of Mechanical Engineering, Department of Robotics, 17. listopadu, 70833, Ostrava-Poruba, tel. (+420) 59 732 3595, e-mail: petr.novak@vsb.cz

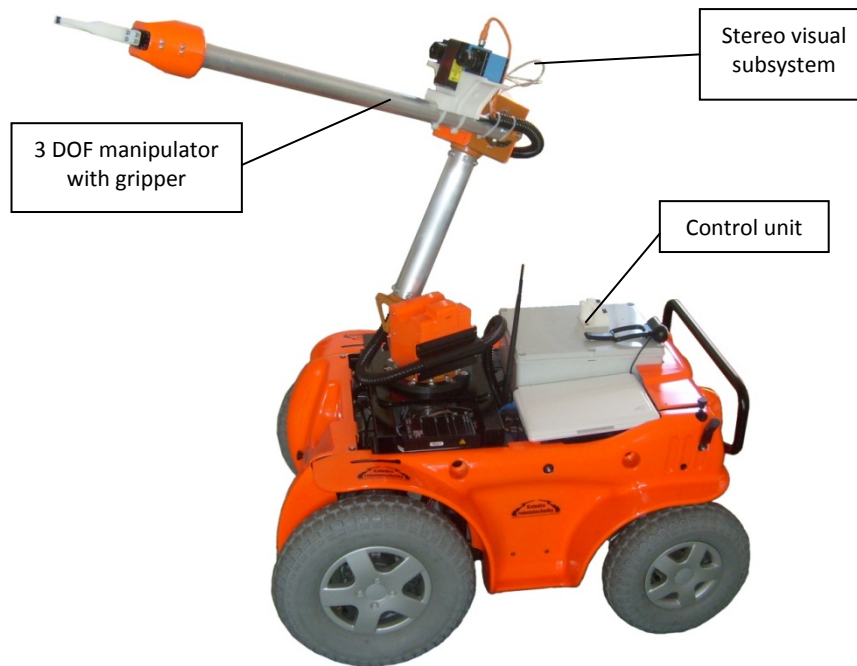


Fig. 1 MR HERCULES

2 MANIPULATION SUBSYSTEM

Manipulator (Fig. 2) designed for the MR HERCULES is characterized by basic technical parameters given in Tab. 1. The Manipulator has angular kinematics structure.

The main problem which has to be solved during mechanical design of a manipulator for a mobile system is an energy source limitation. So the requirement on low energy consumption of all MR subsystems is very important. The nominal voltage is limited to 24 V DC, which is provided by a pair of traction lead accumulators with total capacity of 60 Ah. These accumulators feed all the subsystems of MR. Another logical requirement on the manipulator is the lowest possible mass and low moments of inertia of the manipulator links, while at the same the payload capacity of the manipulator is required to be as high as possible. Next significant requirement is the capability of precise manipulation, which means elimination of backlash in rotational joints of the manipulator. Budget for realization of the manipulation subsystem was also one of the crucial limitations.

The key components of the manipulator are the drive units for rotational joints (see below). The manipulator is equipped with a two-finger parallel gripper with controllable gripping force and with appropriate parameters. It is a standard commercial electrical gripper MITSUBISHI for industrial robots.

Tab. 1 – Manipulator technical parameters

| | |
|------------------------------|---------|
| Weight of the manipulator | 22.2 kg |
| Payload | 2 kg |
| Weight of the gripper | 0.6 kg |
| Max. weight of OM | 1.4 kg |
| Max. reach | 1390 mm |
| Nominal voltage | 24 V DC |
| Degrees of freedom | 3 |
| Drives - 3x MAXON EC90F 60 W | |

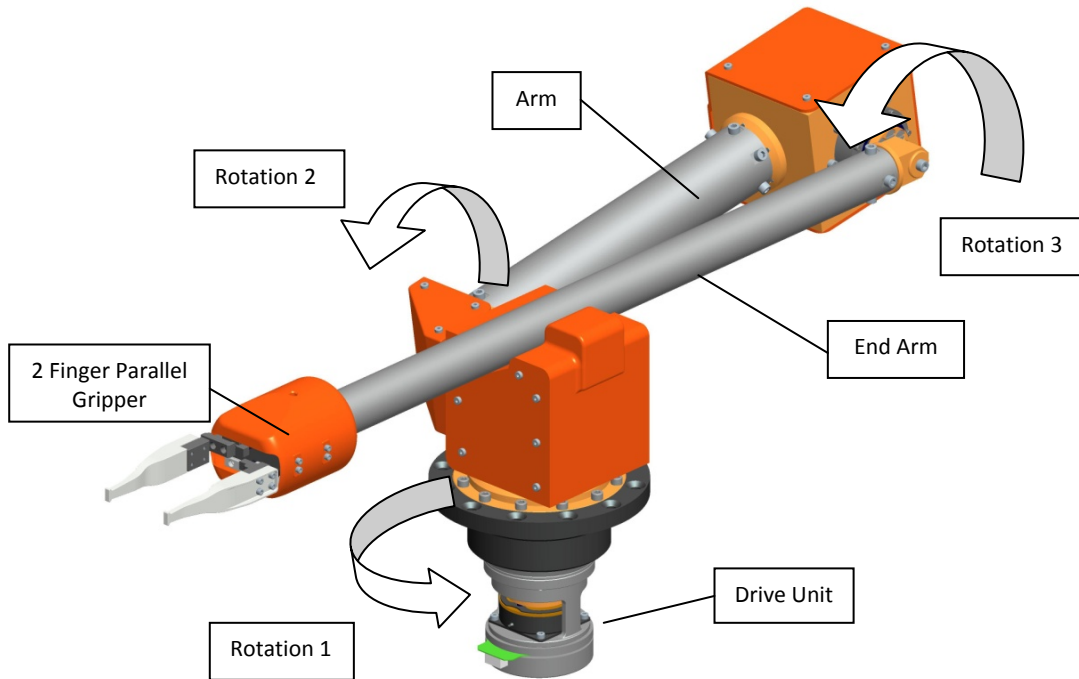


Fig. 2 Manipulation subsystem

3 SERVO DRIVE UNIT

The drive unit (Fig. 3) consists of two principal constituents: a flat MAXON motor EC90F 60 W with encoder and a harmonic unit CSG-20-160-2UH produced by Harmonic Drive AG.

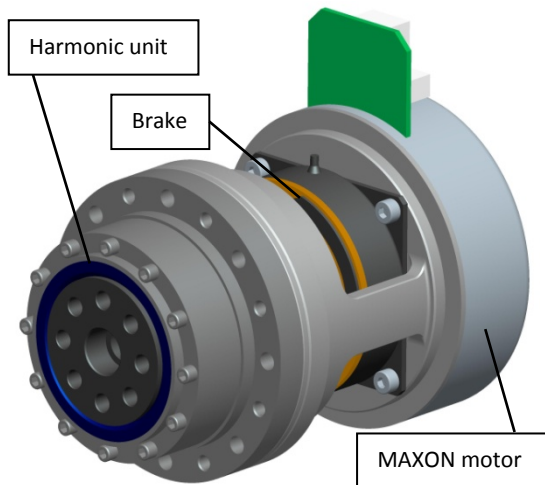


Fig. 3 Servo drive unit



Fig. 4 Assembly of drive units

Identical drive units are used for all three rotational joints, which brought reduction of necessary time of manipulator design as well as production costs.

Usage of identical drive units has a disadvantage – the drive unit for rotational joint ROTATION 3 is too big and strong for its purpose. The unit for this joint could be smaller and lighter. In spite of that, design and especially production of a smaller drive unit would cause significant increase of production costs and also duration of production and assembly. On the other hand, the advantage of this conception is that the manipulator has significantly higher payload capacity in some specific configurations.

Tab. 2 – Drive unit technical parameters

| | |
|--------------------------|-------------|
| Weight of the drive unit | 2.85 kg |
| Nominal output torque | 51 Nm |
| Output RPM | 4.4 rev/min |
| Ratio | 160 |
| Nominal voltage | 24 V DC |

4 ANALYTICAL DETERMINATION OF MANIPULATOR DEFLECTION

Magnitude of manipulator deflection was specified analytically the specific position shown on Fig. 8, for load from the own manipulator mass and from additional load $m_z = 1.5$ kg. Total deflection of the manipulator is the sum of the drive unit torsional displacement and deflections of arms. Drive unit torsional deflection is induced by torsion of Oldham coupler centre disc and harmonic unit flexspline.

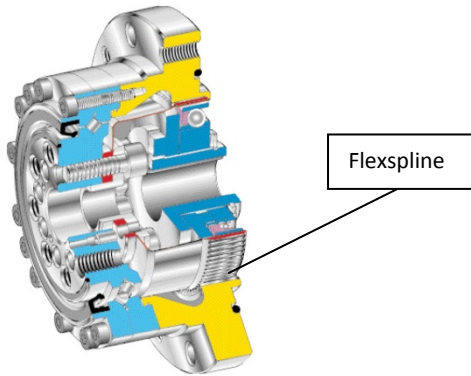


Fig. 5 Harmonic unit CSG-2UH

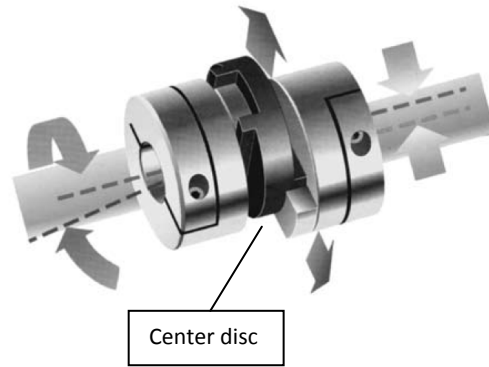


Fig. 6 Oldham coupler

4.1 Torsion displacement of Oldham centre disc

Maximal permissible torque transferred by the drive unit between motor and harmonic unit input is 0.571 Nm. This is the maximal permissible value of the input torque for harmonic unit which was used. Torsional displacement of Oldham coupler centre disc can be specified as:

$$\varphi_{Oldham} = \frac{M_M}{t_K} = \frac{0.571}{115} = 4.9652 \cdot 10^{-3} \text{ rad} = 0.284^\circ, \quad (1)$$

where $M_M = 0.571$ Nm is the maximal transmitted torque on harmonic unit input and $t_K = 115$ Nm/rad is the torsional stiffness of the Oldham OX19G coupler centre disc.

Torsional displacement of harmonic unit output flange (drive unit) φ_{HP} is given as division of the angle φ_{Oldham} and the harmonic unit ratio $i_p = 160$:

$$\varphi_{HP} = \frac{\varphi_{Oldham}}{i_p} = \frac{0.284}{160} = 1.775 \cdot 10^{-3}^\circ, \quad (2)$$

4.2 Torsion displacement of harmonic unit flexspline

For determination of torsion displacement of harmonic unit flexspline it is necessary to evaluate torques acting on outputs of drive units in joints Rotation 2 and 3 of the manipulator in the specified position of arms. A force analysis was made for the given manipulator configuration (Fig. 8) in two situations:

1. without additional load, only load induced by masses of the manipulator arms,
2. with additional load m_z .

Torsion displacement of harmonic unit flexspline for this type of force action is given by a relation which is provided by the unit producer:

$$\varphi_p = \frac{T_1}{K_1} + \frac{T - T_1}{K_2}, \quad (3)$$

where:

T_1 – harmonic unit output torque induced by masses of manipulator arms [Nm],

T – harmonic unit output torque induced by masses of manipulator arms and by the additional load [Nm],

K_1 – stiffness coefficient given by harmonic unit producer $\left[\frac{\text{Nm}}{\text{rad}} \right]$,

K_2 – stiffness coefficient given by harmonic unit producer $\left[\frac{\text{Nm}}{\text{rad}} \right]$.

Angles of torsion displacements were specified using the relation (3). Angles were specified for drive units in manipulator joints Rotation 3 and Rotation 2 in the manipulator configuration shown on Fig. 8

$\varphi_{3p} = 0.0403^\circ$ is the torsion displacement in the joint Rotation 3 drive unit

$\varphi_{2p} = 0.1591^\circ$ is the torsion displacement in the joint Rotation 2 drive unit

And displacement of the manipulator arm end point for both arms is:

$$d_{13p} = 0.605mm$$

$$d_{12p} = 1.250mm$$

4.3 Deflection of manipulator arms

Total deflection of the manipulator is also caused by deflections of manipulators arms induced by action of external forces. These deflections were specified by structural analyses of the manipulator arms, which were made in ANSYS. Deflection caused by additional load of 1.5 kg was specified as a difference between deflection with additional load and deflection without additional load (deflection induced only by own mass of the manipulator).

$$d_{13m} = 0.489mm$$

$$d_{12m} = 0.025mm$$

4.4 Total Deflection of manipulator mechanical components

The deflection induced by torsion displacement of the Oldham coupler centre disc is so small in comparison to the others that it can be ignored during specification of total manipulator arm deflection. The total deflection of the manipulator arm is given as a sum of the deflection induced by the torsion displacement of the harmonic unit flexspline and the deflection induced by mass of the manipulator arm and by mass of the additional load.

$$d_{13} = d_{13p} + d_{13m} = 0.605 + 0.489 = 1.094mm \quad (4)$$

$$d_{12} = d_{12p} + d_{12m} = 1.25 + 0.025 = 1.275mm \quad (5)$$

The total displacement of the manipulator end point was specified graphically (Fig. 7). Total deflections of manipulator arms were put into the diagram and total displacement of the manipulator

end point was specified in the analyzed arms configuration. The total displacement of the manipulator end point is $d_1 = 4.806 \text{ mm}$.

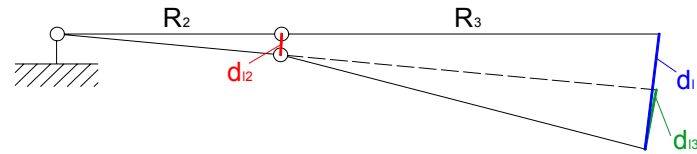


Fig. 7 Total deflection of manipulator

5 EXPERIMENTAL DETERMINATION OF MANIPULATOR DEFLECTION

Measurement methodology of manipulator deflection was designed and realized. Suitably placed laser diodes were used. Their positions are shown on Fig. 8. Principle of the measurement lies in projection of the manipulator deflection (deflections of both arms) on a wall by optical way. If the distance between the manipulator and the wall (measuring plane) is sufficient, displacements of laser points from diode L2 and L3 can be easily measured on the wall. The distance l_d between the wall and the manipulator joint R2 was 5 meters. Described calculation is based on similarity of triangles.

The manipulator is mounted on sprung undercarriage, which induced additional displacement of the manipulator end point. Measure system was supplemented with laser diode L1 to eliminate this additional displacement. Laser diode L1 was placed on the undercarriage. The laser point of diode L1 was the basic reference for the measurement of arms deflections.

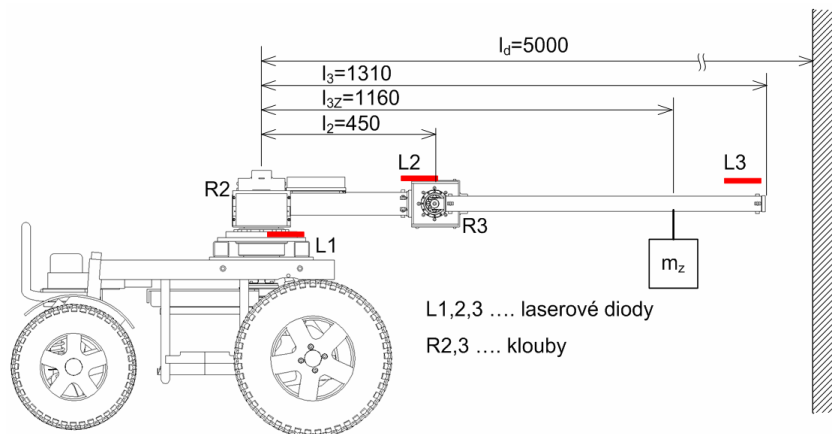


Fig. 8 Measurement of manipulator deflection, positions of laser diodes

The goal of the measurement was specification of deflections of manipulator arms in locations of joints L2 and L3. Also the total displacement of manipulator end point was specified. Results of measured deflections are compared with analytically specified deflections in next chapter.

These measurements were done to obtain needed data:

- Measurement was done by upright position of the manipulator. Goal of the measurement was to find out position of laser diode L1 trace point on the measure plane – red point on Fig. 9. This point was basic reference for other measurements.

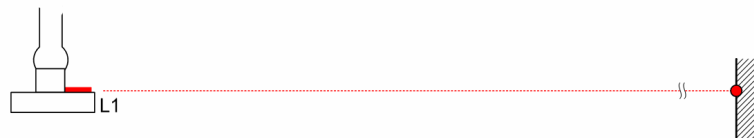


Fig. 9 Basic reference point of laser diode L1

- b) Measurement was done by analyzed horizontal position of the manipulator without additional load $m_z=0\text{kg}$ (Fig 10).

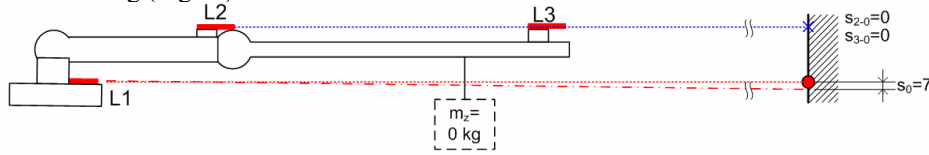


Fig. 10 Additional measurement of undercarriage declination - parameter s_0

An additional parameter s_0 was specified on the basis of this measurement. This parameter determines declination of the undercarriage with manipulator in horizontal position without load m_z . Laser diodes L2 and L3 were set so, that their trace points on the measure plane were in same horizontal plane as it is shown on Fig. 10 (simplification of subsequent measurements). Angle of undercarriage was calculated on the basis of measured parameter s_0 and it is $0,08^\circ$.

- c) Measurement was done by analyzed horizontal position of the manipulator with additional load $m_z=1,5\text{kg}$ (Fig 11).

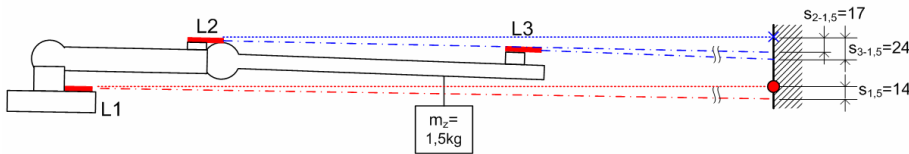


Fig. 11 Measurement of the manipulator deflection induced by load $m_z=1.5\text{kg}$

The additional load m_z with weight 1,5 kg was applied on specified point by this measurement. The additional load produced next declination of the undercarriage (displacement of the Laser 1 point) as well as deflections of manipulator arms indicated by Laser 2 - $s_{2,1.5}=17$ mm and Laser 3 - $s_{3,1.5}=24$ mm. Diagram of the measurement is shown on Fig. 11.

These values of parameters included also the declination of the undercarriage. The declination was eliminated by restatement of the parameter $s_{2,1.5}$ on parameter $s_{E2,1.5}$. Parameter $s_{3,1.5}$ was recalculated on $s_{E3,1.5}$.

Results of the parameters restatement are shown on Fig. 12. The trace point of the L1 laser diode is then in the same position as in case of measurement a) (Fig. 9). Displacement of the laser beam of the diode L2: $s_{E2,1.5} = 10$ mm and L3: $s_{E3,1.5} = 17$ mm is shown on the Fig. 12.

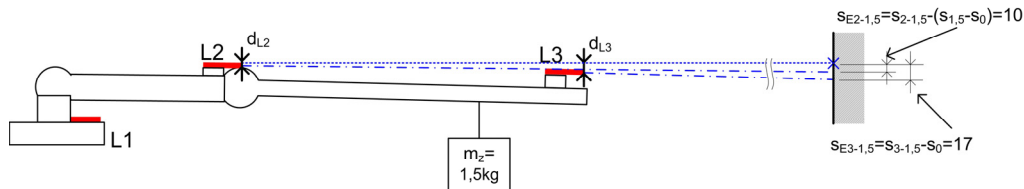


Fig. 12 Measurement of the manipulator deflection induced by load $m_z=1.5\text{kg}$ with restatement for elimination of the undercarriage declination

Displacements of end points of manipulator arms were calculated based on displacements of laser beams of diodes L2 and L3, distance from the measure plane and known dimensions of arms:

Displacement in L2*:

$$d_{L2}^* = l_2 \cdot \tan \alpha_{R2} = l_2 \cdot \frac{s_{E2,1.5}}{l_d} = 450 \cdot \frac{10}{5000} = 0.9\text{mm}, \quad (6)$$

Displacement in L3*: (length of end arm is $l_3 - l_2$)

$$d_{L3}^* = d_{L2}^* + (l_3 - l_2) \cdot \tan \alpha_{R3} = d_{L2}^* + (l_3 - l_2) \cdot \frac{s_{E3-1,5} - d_{L2}^*}{l_d - l_2} = 0.9 + 860 \cdot \frac{17^* - 0.9}{5000 - 450} = 3.94mm, \quad (7)$$

These values (marked by asterisks) were necessary to append with information about accuracy. Values of laser trace points positions measured on measure plane are data with biggest uncertainties of measurements. The trace point of the laser beam on the measure plane had 4 mm in diameter so the position of the point centre couldn't be specified absolutely exactly. The uncertainty of the centre point specification was estimated ± 1 mm. Displacements of manipulator arms end points are:

Displacement in L2:

$$d_{L2} = l_2 \cdot \frac{s_{E2-1,5} \{\pm 1mm\}}{l_d} = 450 \cdot \frac{10 \{\pm 1\}}{5000} = \begin{Bmatrix} 0.81 \\ 0.99 \end{Bmatrix} \cong 0.9 \pm 0.1mm, \quad (8)$$

Displacement in L3:

$$d_{L3} = \begin{Bmatrix} 0.81 \\ 0.99 \end{Bmatrix} + 860 \cdot \frac{s_{E3-1,5} \{\pm 1mm\} - \begin{Bmatrix} 0.81 \\ 0.99 \end{Bmatrix}}{l_d - l_2} = \begin{Bmatrix} 0.81 \\ 0.99 \end{Bmatrix} + 860 \cdot \frac{17 \{\pm 1\} - \begin{Bmatrix} 0.81 \\ 0.99 \end{Bmatrix}}{4550} = \begin{Bmatrix} 3.7 \\ 4.2 \end{Bmatrix} \cong 3.95 \pm 0.25mm, \quad (9)$$

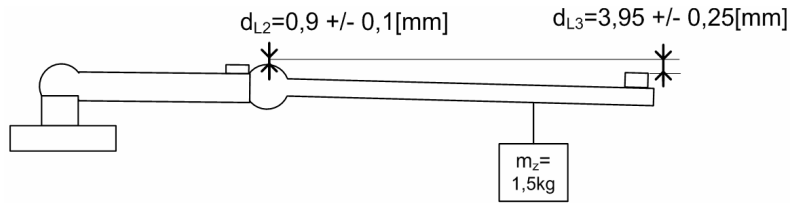


Fig. 13 Graphic interpretation of measurement results

6 COMPARISON OF COMPUTED AND MEASURED VALUES OF DISPLACEMENTS

Tab. 1 Values of arms end points displacements

| Point of displacement | Computed values | Measured values |
|-----------------------|-----------------|-----------------|
| L2 | 1.275 mm | 0.9±0.1 mm |
| L3 | 4.806 mm | 3.95±0.25 mm |

Difference between computed and measured values of displacement in location L2 is 20%. Difference in location L3 is then 25%. Reasons of these differences may be:

The most important parameter for analytically specified displacement of the arm endpoint is the torsion displacement of the harmonic unit which is given by coefficient of the harmonic unit flexspline stiffness. The flexspline stiffness is given by harmonic unit producer for specified type of force action. The producer gives the same value of stiffness coefficient for various types of force action. It is possible, that the value of the coefficient may slightly vary about given value in dependency on conditions of force action. Small change in stiffness coefficient (units of percents) would induce displacement of arm end point in tenths of millimeter.

The difference between computed and measured value of arms end points displacements is within an acceptable range. The measurement was done in our laboratory a we had only provisional equipment. For example usage of laser diodes with better optics would provide more exactly results.

Also the special measuring fixture to eliminate the declination of the undercarriage would increase the measurement accuracy. On the other hand some simplifications were done also by analytic determination of manipulator arms deflections. For verification of our assumptions was the measuring accuracy sufficient.

7 CONCLUSIONS

The manipulation subsystem of the HERCULES mobile robot was described in the article. The drive unit designed for the manipulator was also described. In the next chapter the analytic calculation of the manipulator end point total displacement was presented. The methodology of measurement which was made to verify the calculated values of arms displacements and the comparison of calculated and measured values was presented as well.

This article was compiled as part of projects FT-TA3/014, supported by the Fund for University Development from the Ministry of Industry and Trade.

REFERENCES

- [1] MOSTÝN V., SKAŘUPA J. *Teorie průmyslových robotů*. 1st ed. Košice: Viena Košice, 2000, 146 pp. ISBN 80-88922-35-6.
- [2] MOSTÝN V., NOVÁK P., KOT T., MIHOLA M., KRYS V. Simulation model of manipulating arms of the service robot. *Metallurgy*. 2010, vol. 49. Nr. 2, pp. 393-399. ISSN 0543-5846.
- [3] HARMONIC DRIVE AG. *CSF & CSG Series*. rev 03-06. 800-921-3332, 50 pp.
- [4] HARMONIC DRIVE AG. *Assembly and Service Manual – CSG-2UH Series Units*. 900149 01/2006, 20 pp.
- [5] MAXON MOTOR. *High Precision Drives and Systems - Program 09/10*. 361 pp.

